

RESEARCH

Open Access



Transcriptomics-based exploration of ubiquitination-related biomarkers and potential molecular mechanisms in laryngeal squamous cell carcinoma

Qiu Chen^{1,2}, Zhimin Wu¹ and Yifei Ma^{2*}

Abstract

Background One of the most common and prevalent cancers is laryngeal squamous cell carcinoma (LSCC), which poses a great threat to the life and health of the patient. Nonetheless, it has been demonstrated that ubiquitination is crucial for the development and course of LSCC. Therefore, it is particularly important to identify biomarkers for ubiquitination-related genes (UbRGs) in LSCC.

Methods Differentially expressed genes (DEGs) in the LSCC versus controls were obtained by differential expression analysis. Also, key modular genes associated with LSCC were obtained using weighted gene co-expression network analysis (WGCNA). Next, DEGs, key module genes, and UbRGs were taken to intersect to obtain candidate genes. And then machine algorithms were to screen potential biomarkers, further their diagnostic value were analyzed and validated. Then, therapeutic agents for biomarkers were predict. In addition, the regulatory networks of the biomarkers were mapped. The expression levels of biomarkers were detected in clinical samples using reverse transcription-quantitative PCR (RT-qPCR).

Results A total of eight candidate genes were acquired by the overlap 1,911 DEGs, the key modular genes of WGCNA, and 1,393 UbRGs. A sum of four biomarkers (WDR54, KAT2B, NBEAL2 and LNX1) were identified by two machine learning, then these four biomarkers were validated in GSE127165 and the expression trend was consistent with TCGA-LSCC, they were recorded as biomarkers. Moreover, the accuracy of the biomarkers in predicting clinical aspects of LSCC was confirmed by the receiver operating characteristic (ROC) curves. Subsequently, cancers such as malignant neoplasms, colorectal cancers, tumors, and primary malignant neoplasms were significantly associated with the biomarkers, which further suggests that these four biomarkers were strongly associated with cancer. Meanwhile, the drugs garcinol, cocaine, and triazolam, among others, used for LSCC treatment were predicted. Finally, transcription factors (TFs) (BRD4, MYC, AR, and CTCF) were predicted to regulate the biomarkers. RT-qPCR assays illustrated that the expression trends of KAT2B, LNX1 and NBEAL2 remained consistent with the dataset.

*Correspondence:

Yifei Ma
mayifei@gmc.edu.cn

Full list of author information is available at the end of the article



© The Author(s) 2025. **Open Access** This article is licensed under a Creative Commons Attribution-NonCommercial-NoDerivatives 4.0 International License, which permits any non-commercial use, sharing, distribution and reproduction in any medium or format, as long as you give appropriate credit to the original author(s) and the source, provide a link to the Creative Commons licence, and indicate if you modified the licensed material. You do not have permission under this licence to share adapted material derived from this article or parts of it. The images or other third party material in this article are included in the article's Creative Commons licence, unless indicated otherwise in a credit line to the material. If material is not included in the article's Creative Commons licence and your intended use is not permitted by statutory regulation or exceeds the permitted use, you will need to obtain permission directly from the copyright holder. To view a copy of this licence, visit <http://creativecommons.org/licenses/by-nc-nd/4.0/>.

Conclusion The identification of four biomarkers (WDR54, KAT2B, NBEAL2 and LNX1) associated with UbRGs could ultimately serve as a predictive clinical diagnosis of LSCC and provide insight into the molecular mechanisms of LSCC.

Keywords Laryngeal squamous cell carcinoma, Ubiquitination-related genes, WGCNA, Biomarkers, Regulatory network

Introduction

Laryngeal squamous cell carcinoma (LSCC) refers to malignant tumors occurring in the squamous cells of the larynx, and is the most common type of laryngeal cancer with highly aggressive and easily metastasized characteristics. Pathological features of LSCC include cellular anisotropy, nuclear pleomorphism, and irregular proliferation patterns. The LSCC main risk factors include long-term smoking, excessive alcohol consumption, occupational chemical exposure and human papilloma-virus (HPV) infection, occupational exposure, dietary habits, gastroesophageal reflux disease, genetic factors, and immune system status, etc [1]. Definitive diagnosis of laryngeal cancer usually requires a combination of clinical symptoms, imaging, endoscopy, and pathologic testing, and the gold standard for diagnosis is pathologic biopsy. Therapeutic options for LSCC include surgical treatment, radiotherapy, chemotherapy, targeted therapies, and immunotherapy, etc. However, due to its nonspecific pathogenesis, about 60% of patients are in advanced stages at the time of diagnosis and have a low 5-year survival rate [2]. This imposes a heavy financial burden on patients and seriously affects the survival rate of LSCC patients. Therefore, there is an urgent need to identify new biomarkers for LSCC and explore new effective therapeutic targets to improve its survival.

Ubiquitination is an important intracellular protein modification process that involves covalently attaching small protein to target proteins, thereby tagging them for degradation or regulating their function [3]. In the development and progression of laryngeal squamous cell carcinoma (LSCC), ubiquitination plays a key role in regulating tumor suppressors and oncogene stability. It has been shown that microtubule cross-linking factor 1 circRNA (circMTCL1, circ0000825) plays a critical oncogenic function in laryngeal carcinogenesis and progression by promoting complement C1q-binding protein (C1QBP)-dependent ubiquitin degradation, which in turn activates Wnt/ β -catenin signaling [4]. USP21 plays a critical oncogenic function in laryngeal carcinogenesis and progression by de-ubiquitinating and stabilizing AURKA. Wang QD [5] et al. demonstrated that USP21 stabilized AURKA through deubiquitination, thereby promoting laryngeal cancer progression. Current research on ubiquitination-related genes in laryngeal squamous cell carcinoma (LSCC) remains limited, particularly in elucidating the precise roles of ubiquitination modifications during LSCC pathogenesis and progression. Although several

studies have revealed potential functions of specific E3 ubiquitin ligases and deubiquitinating enzymes in LSCC, these investigations have primarily focused on individual genes or isolated pathways, lacking systematic and comprehensive analyses. The current understanding of ubiquitination-associated regulatory networks and their complex mechanisms within the tumor microenvironment remains insufficient. Therefore, there is an urgent need for more in-depth studies on ubiquitination-related genes and their molecular mechanisms in LSCC, which could provide more reliable theoretical foundations and practical guidance for early diagnosis, prognostic evaluation, and targeted therapy of this malignancy.

In this study, we explored the association between ubiquitination-related genes (UbRGs) and LSCC based on bioinformatics analysis, and explored the potential of UbRGs as a biomarker for LSCC through public data acquisition, differential expression analysis, functional enrichment analysis, survival analysis, and oncogenic pathway analysis. We will explore the potential of UbRGs as biomarkers of LSCC and their potential molecular mechanisms through public data acquisition, differential expression analysis, survival analysis, and oncogenic pathway analysis, and validate the expression of key genes in the population, with the aim of gaining a deeper understanding of the pathogenesis and therapeutic targets of LSCC.

Materials and methods

Data source

TCGA-LSCC was obtained from the Cancer Genome Atlas (TCGA) as a training set. It included RNA-seq data, overall survival (OS), and clinical information for 116 laryngeal squamous cell carcinoma (LSCC) tumour tissue samples and 12 paracancerous tissue samples. The GSE127165 and GSE27020 datasets were downloaded from the Gene Expression Omnibus (GEO) database. The GSE127165 (platforms: GPL20301) dataset was used as a validation set for biomarker expression and clinical diagnostic capabilities, including 57 LSCC and 57 paracancerous tissues [6]. The GSE27020 (platforms: GPL96) dataset was used for survival analysis validation of LSCC and includes disease-free survival (DFS), clinical information, and tissues of 109 LSCC patients [7]. Detailed information on the three datasets can be found in Table 1. A total of 1,393 ubiquitination-related genes (UbRGs) were obtained from the integrated annotations for Ubiquitin

Table 1 Detailed information of datasets

Accession ID	Platform name	Platform ID	Number of samples	Publication date
GSE127165	Illumina HiSeq	GPL20301	LSCC tissues (57 samples) and paired adjacent normal mucosa tissues (57 samples)	2020/6/17
GSE27020	Affymetrix GeneChip	GPL96	109 LSCC tumor tissue samples	2013/10/30

and Ubiquitin-like Conjugation database (iUUCD2.0). The flow chart of this study is shown in Fig. 1.

Selection of candidate genes

The Benjamini-Hochberg method was used to adjust the raw p-values for FDR, and significant differentially expressed genes were selected based on the adjusted p-values ($p_{adj} < 0.05$). The ‘DESeq2’ ($|\log_2\text{fold-change (FC)}| > 2$, $p\text{-value} < 0.05$) (version 1.36.0) [8] was used to identify differentially expressed genes (DEGs) between LSCC and controls. In the meantime, the key modules most relevant to LSCC were obtained by weighted gene co-expression network analysis (WGCNA) [9] using the ‘WGCNA’ (version 1.72-1). In the first instance, the samples in TCGA-LSCC were clustered, and outlier samples were removed. And the soft threshold was applied to guarantee a scale-free network (a scale-free R^2 near 0.9). Then, similarly expressed genes were grouped into identical gene modules using the dynamic tree-cutting method.

Next, the dynamic tree-cutting method was used to group genes that were expressed similarly into gene modules that were identical. Then, the module with the highest correlation to LSCC was selected as the key module. Immediately after, the candidate genes were obtained by taking the intersection of the DEGs with the key module genes and the three parts of the UBRGs. Finally, the biological functions as well as signalling pathways in which the candidate genes were involved were obtained by the ‘clusterProfiler’ (version 4.0.2) [10].

Identification of biomarkers as well as clinical diagnoses

Firstly, the log-likelihood values of different models were calculated, and the Likelihood Ratio Test was used to evaluate the performance of the different models. The candidate genes were screened predicate the optimal coefficients and values of lambda utilising the ‘glmnet’ (version 4.1-4) [11] to proceed the Least Absolute Shrinkage and Selection Operator (LASSO) analysis [12] to obtain potential biomarkers. Next, the candidate genes for specific variables associated with LSCC results were screened via Boruta algorithm according to ‘Boruta’ (version 7.0.0) [13] as potential biomarkers for LSCC. Immediately after that, the intersection of LASSO and Boruta results were taken to obtain biomarkers for LSCC. Then, biomarkers with consistent expression in the TCGA-LSCC and GSE127165 datasets were screened for subsequent analyses. Finally, the ability of the biomarkers to diagnose LSCC was assessed using the receiver operating characteristic (ROC) curves of ‘pROC’ (version 1.18.0)

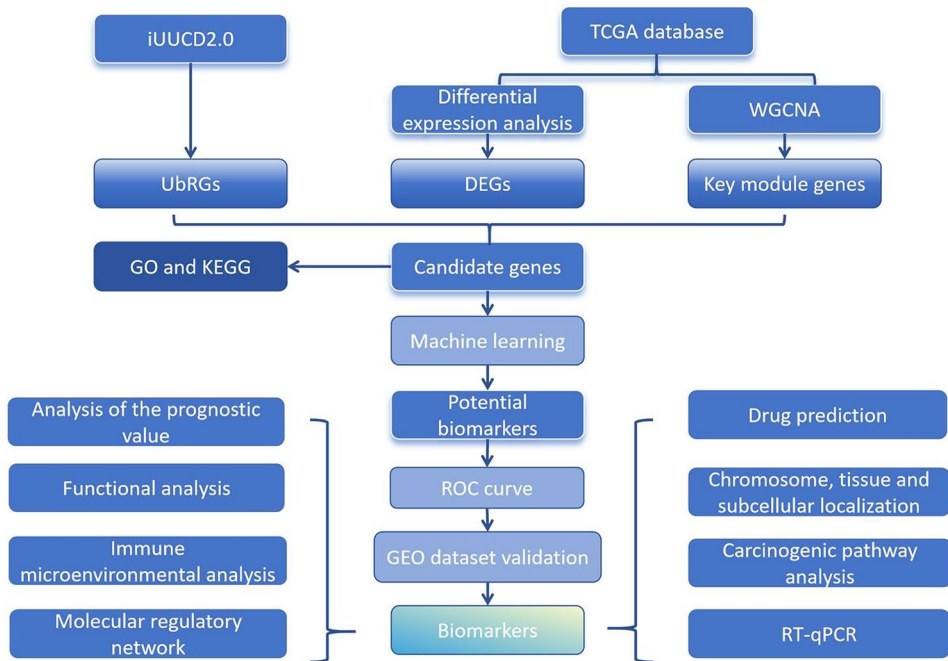


Fig. 1 The flow chart of this study

[14]. And the closer the area under curve (AUC) was to 0.7, the better the biomarker's ability to diagnose LSCC in the clinic.

Analysis of the prognostic value of biomarkers

Survival analyses for OS and DFS were performed on the prognostic value of the biomarkers, and the LSCC samples were divided into two groups (high and low expression groups) according to the optimal threshold of biomarker expression award. And then the 'survminer' (version 0.4.9) [15] was applied to perform Kaplan-Meier (K-M) survival curves to observe the biomarkers affecting the survival differences between different expression groups. At the same time, differences in biomarkers across expression groups were validated in the GSE27020 dataset. Additionally, the Wilcoxon test was used to compare the biomarker expression in these clinical characteristics (gender, age, TNM stage, and stage) based on the clinical characteristics found in the TCGA-LSCC dataset (p -value < 0.05). Next, biomarker expression and clinical characteristics were incorporated into the risk model for univariate Cox independent prognostic analysis. Subsequently, factors with p -values less than 0.05 were screened for subsequent multifactorial Cox independent prognostic analysis to identify independent prognostic factors for LSCC.

Localisation of biomarkers on chromosomes, sub-cells and tissues

The distribution of biomarkers on the human chromosome was analyzed using the 'RCircos' (version 1.2.2) [16]. At the same time, the information about the biomarkers was imported into the Genecards database [17], and the locations of the biomarkers with high subcellular expression were selected using Confidence = 2 as the screening condition. Similarly, to explore the expression of biomarkers at the tissue and organ level, biomarkers were entered into the BioGPS database [18] and retrieved to obtain the distribution of biomarkers in tissues and organs. The mean value of biomarkers in each tissue was also calculated, and organs and tissues with biomarker expression higher than the overall mean were selected.

Functional analysis of biomarkers

The Gene-Gene Interaction (GGI) network of biomarkers was constructed based on GeneMANIA (<http://genemania.org>), and the top 20 interactions with biomarkers were selected for display. Subsequently, in order to understand the relevant biological functions as well as the signaling pathways in which the biomarkers were involved. Gene ontology (GO) functional annotation of biomarkers was performed using the 'clusterProfiler' (version 4.0.2). Meanwhile, the signalling pathways involved in the biomarkers were analysed after the Kyoto Encyclopedia of

Genes and Genomes (KEGG) using the 'org.Hs.eg.db' (version 3.13.0) [19]. Afterwards, similarities between biomarkers GO functions were explored with the help of the 'GOSemSim' (version 2.18.1) [20].

Immune microenvironmental analysis of LSCC

Firstly, the CIBERSORT algorithm was used to calculate the percentage abundance of 22 immune cells for each sample between LSCC and controls in the TCGA-LSCC dataset. After that, the correlation of immune cells occupancy was analysed based on the results using the Spearman. Next, samples with a p -value of less than 0.05 were selected and differences in immune cell infiltration between LSCC and control were analysed using the Wilcoxon test. Similarly, correlations between biomarkers and immune cells were analysed using the Spearman.

Potential cancer-related pathways of biomarkers, related diseases and predictive analysis of targeted drugs

To understand the cancer-related pathways in which biomarkers were involved, biomarkers and cancer-related pathways were analyzed using GSCALite databases [21]. At the same time, the Disease Gene Network (DisGeNET) database was used to explore the related diseases that the biomarkers were associated with [22]. Also, in order to find patient-specific therapeutic agents, interactions between biomarkers and targeted drugs were predicted through the GeneCards database [23]. Further, the molecular docking of drug components and biomarker-encoded proteins was explored through 'AutoDock' (version 4.2.6) [24].

Construction of potential regulatory networks for biomarkers

In order to analyze the role that biomarkers play in the regulation of LSCC by expression at the molecular level, it was necessary to perform regulatory network analysis of biomarkers. In the first place, miRNAs regulating biomarkers were predicted in the miRWalk [25] database. Subsequently, common miRNAs in the miRWalk and miRDB [26] databases were combined as miRNAs that regulate biomarkers. Meanwhile, lncRNAs regulating miRNAs were obtained in miRTarBase [27] and tarbase databases [28]. And, the competing endogenous RNA (ceRNA) network of LSCC was constructed. ceRNA can alter the function of target miRNAs by competing for shared binding sites on the miRNA, and lncRNAs can act as ceRNAs to regulate the expression of target mRNAs by competing for shared miRNAs [29, 30]. To understand the regulatory role of biomarkers in cancer, transcription factors (TFs) of biomarkers were also searched with the help of Cistrome [31] database.

Reverse transcription-quantitative polymerase chain reaction (RT-qPCR)

The expression of these biomarkers was validated via RT-qPCR. The 8 control and 7 LSCC tissue samples were obtained from Affiliated Hospital of Guizhou Medical University. All participants provided informed consent, and ethics approval for this study was obtained from the Medical Science Ethics Committee of Affiliated Hospital of Guizhou Medical University, approval number: 2022 (221). Laryngeal cancer and paraneoplastic specimens were obtained from patients who were hospitalized for surgery in the Affiliated Hospital of Guizhou Medical University from 2023.10 to 2024.10. All patients were pathologically diagnosed as laryngeal squamous cell carcinoma, and none of them underwent preoperative radiotherapy. All patients were pathologically diagnosed with laryngeal squamous cell carcinoma, and none of them underwent preoperative radiotherapy. Following the manufacturer's protocol, total RNA was extracted from the 15 tissue samples using TRIzol reagent (Invitrogen, China). Afterwards, RNA concentrations were detected with NanoPhotometer N50. Next, cDNA was obtained via reverse transcription using SureScript-First-strand-cDNA-synthesis-kit (Servicebio, China). The reaction was performed on 40 cycles under the following conditions: pre-denaturation at 95 °C for 1 min, denaturation at 95 °C for 20 s, annealing at 55 °C for 20 s, and extension at 72 °C for 30 s. The relative quantification of mRNAs was computed using the $2^{-\Delta\Delta CT}$ method. The P-value was determined by plotting the data using GraphPad Prism 5. The sequences of all primers could be found in Table 2.

Statistical analysis

This study was conducted using the R programming language (version 4.3.1), and P-values less than 0.05 were considered statistically significant, unless otherwise stated.

Table 2 Primer sequence list

Primers	Sequences
KAT2B F	CGGGCCAAGAACTGGAGA
KAT2B R	TCCAGGTGGGAAACATGAGC
LNX1 F	CCCAGACAGTCGCTTGAAGA
LNX1 R	GGTTCAGGATCGTTGGCAGA
NBEAL2 F	TTGCCCATGGAACCGCTC
NBEAL2 R	GAAGAGCTTGAGCAGCAGGA
WDR54 F	CGTGCGTCGTCTCTATGGTG
WDR54 R	AACATCCTGTGTGGGGGTGC
Internal reference-GAPDH F	CGAAGGTGGAGTCAACGGATT
Internal reference-GAPDH R	ATGGGTGGAATCATATTGGAAC

Results

Acquisition of eight candidate genes

These 1,911 DEGs were obtained from LSCC and controls. Among them, 1,187 DEGs were up-expressed, while 724 DEGs were down-expressed (Fig. 2A). A heatmap illustrated that these DEGs were distributed across the various groups (Fig. 2B). The WGCNA results show that the scale-free R2 can only approach the 0.9 threshold when the soft threshold β was 6 (Fig. 2C). Based on the above, there were 14 co-expressed gene modules indicated by different colours (Fig. 2D). Also, since the blue module has the most significant negative correlation with LSCC ($r = -0.61$, $p\text{-value} < 0.0001$) and the yellow module had the most significant positive correlation with LSCC ($r = 0.54$, $p\text{-value} < 0.0001$), both of these modules were key modules for LSCC (Fig. 2E). The list of genes corresponding to each module is shown in additional file 1. The 1,354 key genes contained in the blue module and 941 key genes contained in the yellow module were used for subsequent analyses. Eight candidate genes (KAT2B, LNX1, NBEAL2, PDLIM2, RNF222, RNFT2, UCHL1, and WDR54) were obtained by intersecting 1,911 DEGs, key module genes, and 1,311 UBRGs (Fig. 2F). Among them, the yellow module has no intersecting genes with DEGs and UBRGs. This suggested that the genes in the yellow module may influence clinical features through other mechanisms (such as regulatory networks or other signaling pathways), rather than solely relying on overlap with DEGs or UBRGs. Functional as well as signalling pathway results of candidate gene enrichment showed that these candidate genes were significantly associated with 'negative regulation of protein serine/threonine kinase activity', 'ubiquitin protein transferase activity', and 'histone acetylation' these functions ($p\text{-value} < 0.05$). And the candidate genes were also involved in 'notch signaling pathway', 'viral life cycle-HIV-1', 'thyroid hormone signaling pathway', and 'viral carcinogenesis' these signalling pathways (Fig. 2G-H).

Four biomarkers with clinical diagnostic capability for LSCC

There were five potential biomarkers (WDR54, UCHL1, KAT2B, NBEAL2, and LNX1) with diagnostic significance for LSCC that were screened by LASSO regression analysis (Fig. 3A-B). Then the Boruta algorithm filtered out seven potential biomarkers (KAT2B, NBEAL2, PDLIM2, WDR54, LNX1, RNF222, and RNFT2) of important candidate feature genes (Fig. 3C). WDR54, KAT2B, NBEAL2 and LNX1 were the four biomarkers that emerged from the combination of the results of the Boruta and LASSO screening (Fig. 3D). Subsequently, the expression of these four biomarkers in the GSE127165 dataset was consistent with the TCGA-LSCC dataset. Among them, KAT2B, LNX1, and NBEAL2 were significantly under-expressed in LSCC ($p\text{-value} < 0.0001$),

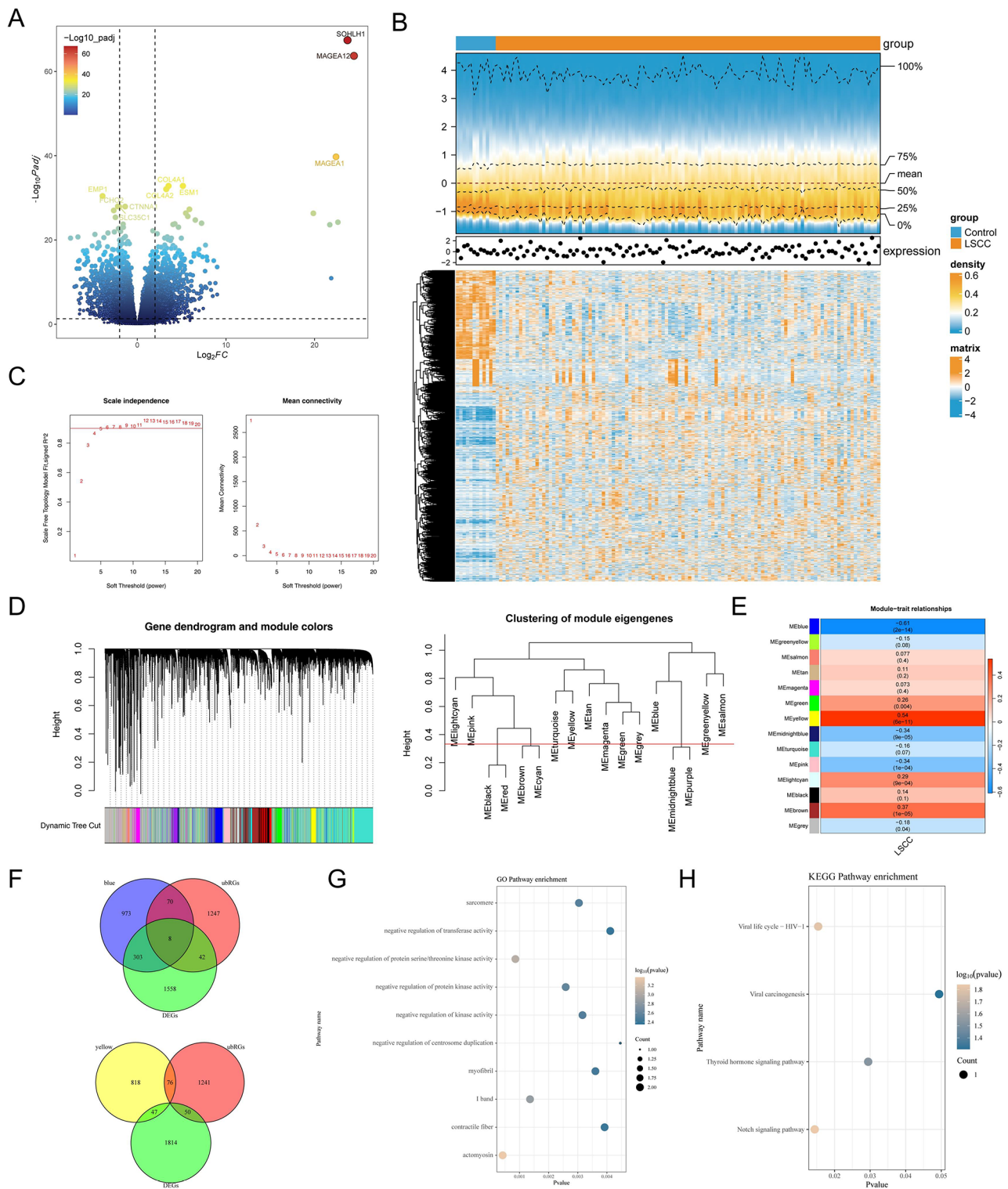


Fig. 2 (A) Differential gene volcano map between laryngeal squamous cell carcinoma (LSCC) and Control groups. (B) Heat map of differential genes between LSCC and Control groups. (C) Selection of power values. (D) Module clustering dendrogram. (E) Heat map of the relationship between gene modules and traits using LSCC as a phenotype. (F) Venn diagram for screening ubiquitination-related differential genes. (G-H) Functional enrichment results for candidate genes

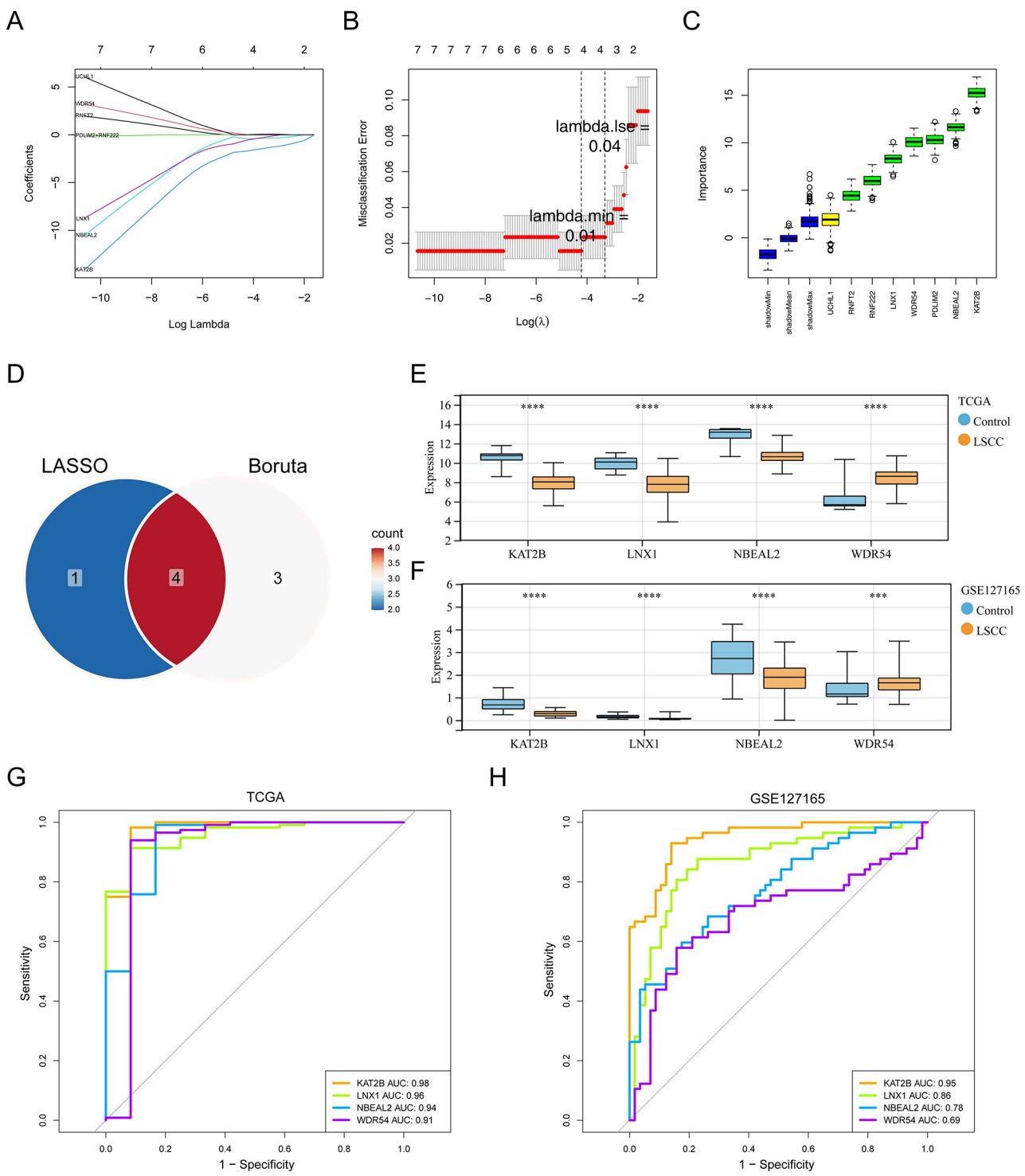


Fig. 3 (A–B) LASSO regression analysis to screen for signature genes. (C) Boruta’s algorithm identifies key genes. (D) Two machine learning algorithms for screening key genes in Wayne diagrams. (E–F) Expression of key genes in different datasets. (G–H) ROC plots for key genes in different datasets

and only WDR54 was significantly over-expressed in LSCC (p-value < 0.001) (Fig. 3E-F). WDR54 (AUC = 0.91), KAT2B (AUC = 0.98), NBEAL2 (AUC = 0.94) and LNX1 (AUC = 0.96) had clinical diagnostic ability of LSCC in the TCGA-LSCC dataset and validated in dataset GSE127165 (AUC was close to 0.7) (Fig. 3G-H).

Prognostic survival analysis of LSCC fulfilled by LNX1

The prognostic analysis of biomarkers revealed that only LNX1 exhibited a statistically significant difference between the expression groups (p-value = 0.046), suggesting that LNX1 may have a potential role in prognosis. While the K-M curves of KAT2B (p-value = 0.096) and WDR54 (p-value = 0.065) could be seen to differ between expression groups with p-values close to 0.05. However, since these p-values do not meet the standard threshold for statistical significance, further investigation with larger sample sizes or additional validation studies would be necessary to determine whether these trends are meaningful and reflect true differences, or if they might be due to random variation. NBEAL2 was not associated with the prognosis of patient (p-value = 0.410) (Fig. 4A-D). Subsequently, it was verified in the GSE27020 dataset that LNX1 was significantly differential (p-value = 0.010) in different expression groups (Fig. 4E).

Gender and cancer status were identified as independent prognostic factors for LSCC

Differences between biomarkers and clinical characteristics showed that LNX1 and NBEAL2 presented significant differences in different N stages and stages, while WDR54 presented significant differences in different N stages (Fig. 5A-E). The univariate Cox results suggested that cancer status, gender, new tumor event, and WDR54 could be relevant independent prognostic factors for LSCC (p-value < 0.05) (Fig. 5F). Subsequently, gender and cancer status could be used as independent prognostic factors for LSCC after further multifactorial Cox screening (p-value < 0.05) (Fig. 5G). These findings suggest a potential relationship between these variables and prognosis.

Biomarker chromosome mapping and construction of subcellular biomarker networks and tissue biomarker networks

Both KAT2B and NBEAL2 were located on human chromosome 3. Human chromosomes 2 and 4 were the locations of WDR54 and LNX1, respectively (Fig. 6A). Biomarkers were highly expressed in subcellular co-locations nucleus, cytoskeleton, plasma membrane, mitochondrion, cytosol, and endoplasmic reticulum (Fig. 6B). In the vast majority of tissues, all four biomarkers were expressed (Fig. 6C).

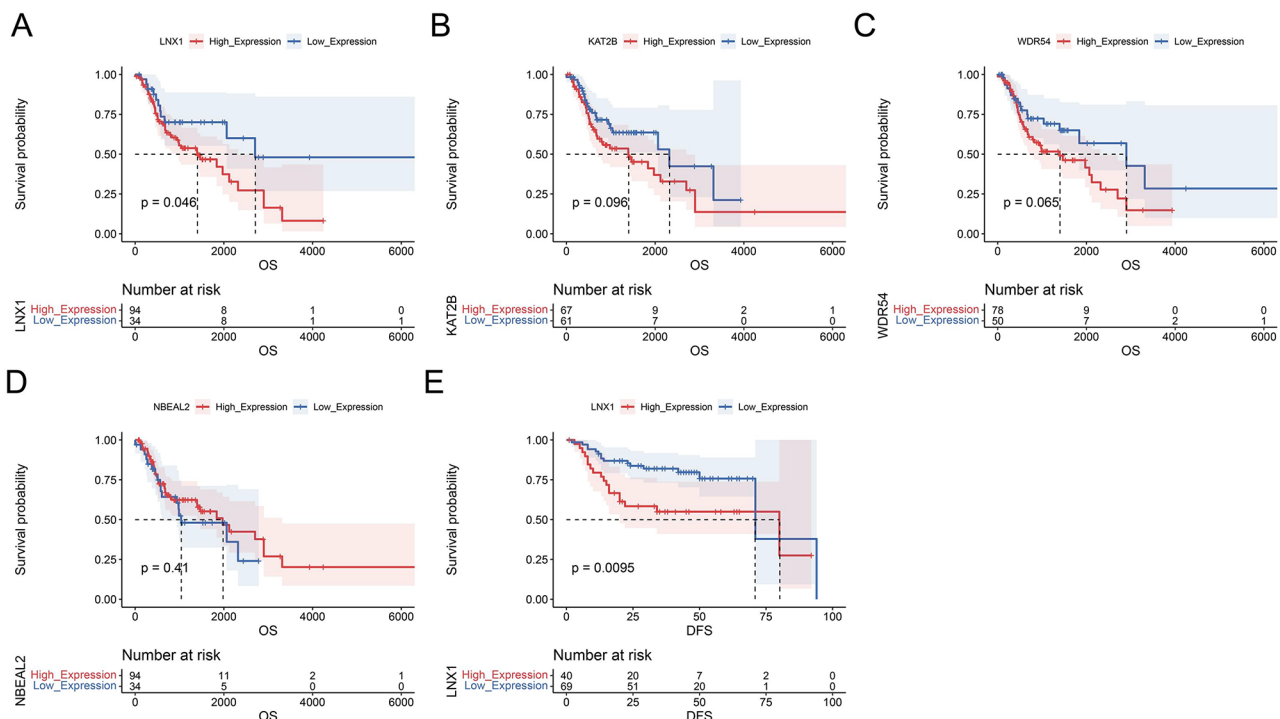


Fig. 4 (A-D) KM curves of high and low expression groups in TCGA-LSCC dataset. (E) KM curves of high and low expression groups in GSE27020 dataset

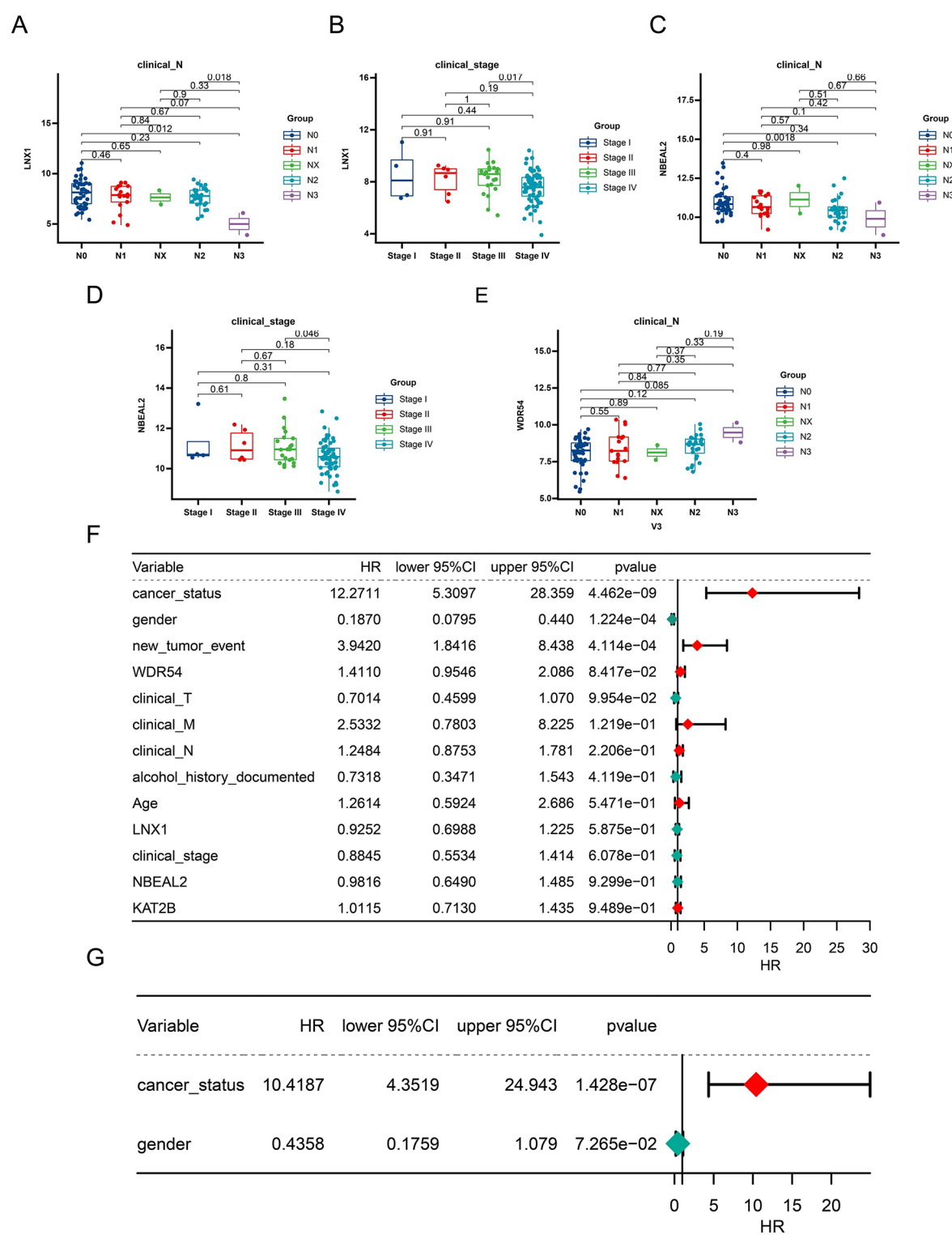


Fig. 5 (A-E) Expression of biomarkers in different clinical traits. (F) Univariate Cox forest plot for independent prognostic analysis. (G) Multifactorial Cox forest plot for independent prognostic analysis

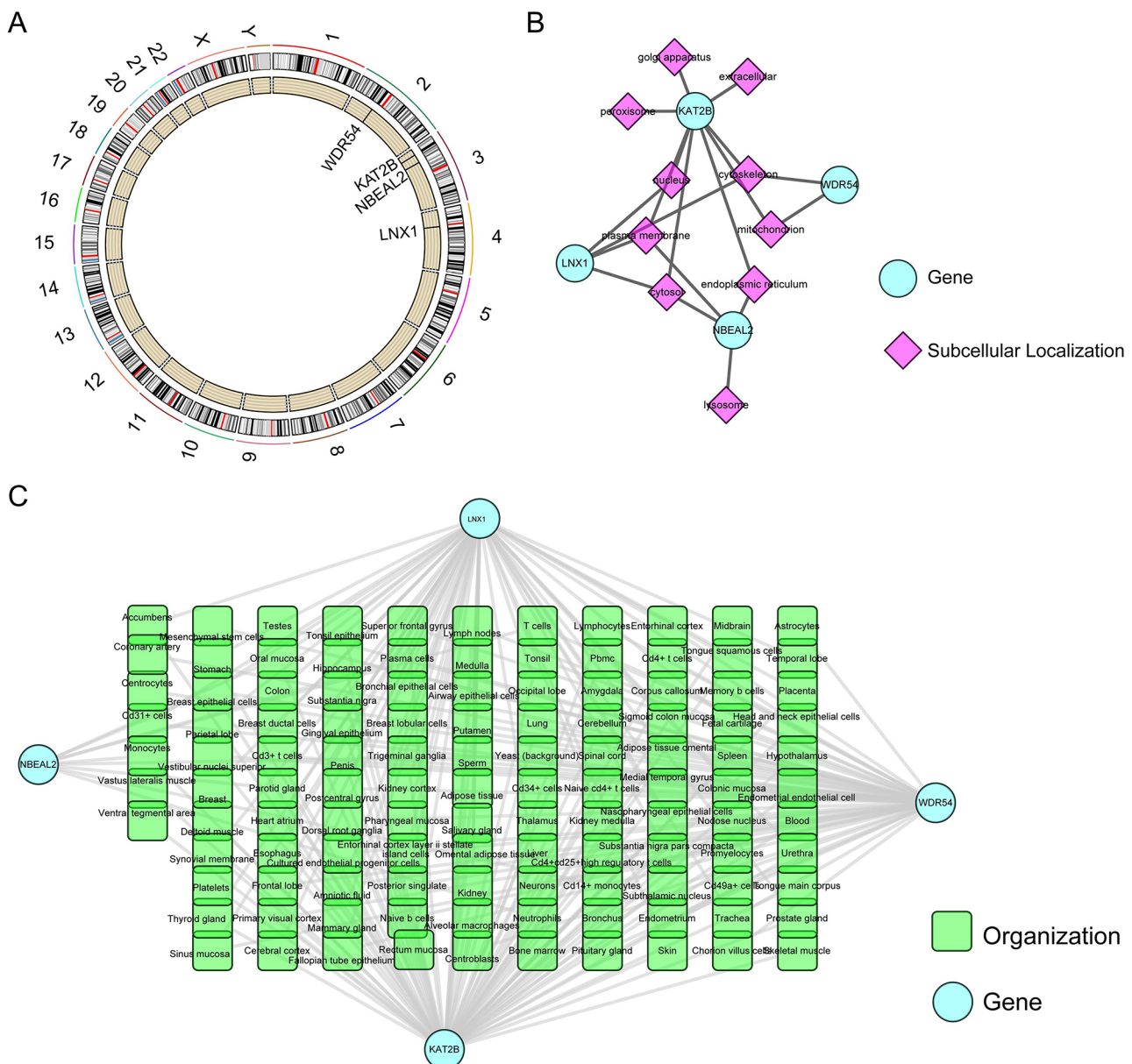


Fig. 6 (A) Distribution of biomarkers on chromosomes. (B) Subcellular localisation network diagram of biomarkers. (C) Tissue-biomarker network diagram

Potential biological functions of biomarkers

There were various relationships between biomarkers and other genes in the GGI network, such as co-expression, same location, physical interactions, genetic interactions, sharing protein structural domains, or involvement in the same pathway (Fig. 7A). The GO results showed that all biological functions involved in KAT2B were inhibited (Fig. 7B). Collagen trimer, in which LNX1 and NBEAL2 were jointly involved, was inhibited (Fig. 7C-D). Cornification and epidermal cell differentiation, in which NBEAL2 was involved and activated, whereas these were inhibited in WDR54 (Fig. 7D-E). Proteasome and ribosome were shown to be inhibited in KEGG results for

KAT2B and LNX1 (Fig. 7F-G). Xenobiotic metabolism of cytochrome P450, drug metabolism of cytochrome P450, adrenergic metabolism, and arachidonic acid metabolism were activated in NBEAL2, whereas these were inhibited in WDR54 (Fig. 7H-I). Immediately following this, the similarity results between biomarkers showed the strongest functional similarity between LNX1, NBEAL2, and KAT2B (Fig. 7J).

Immune infiltration of LSCC

Immune cell infiltration in different samples was shown by heatmap (Fig. 8A). In this case, memory-resting CD4 T cells were significantly negatively correlated

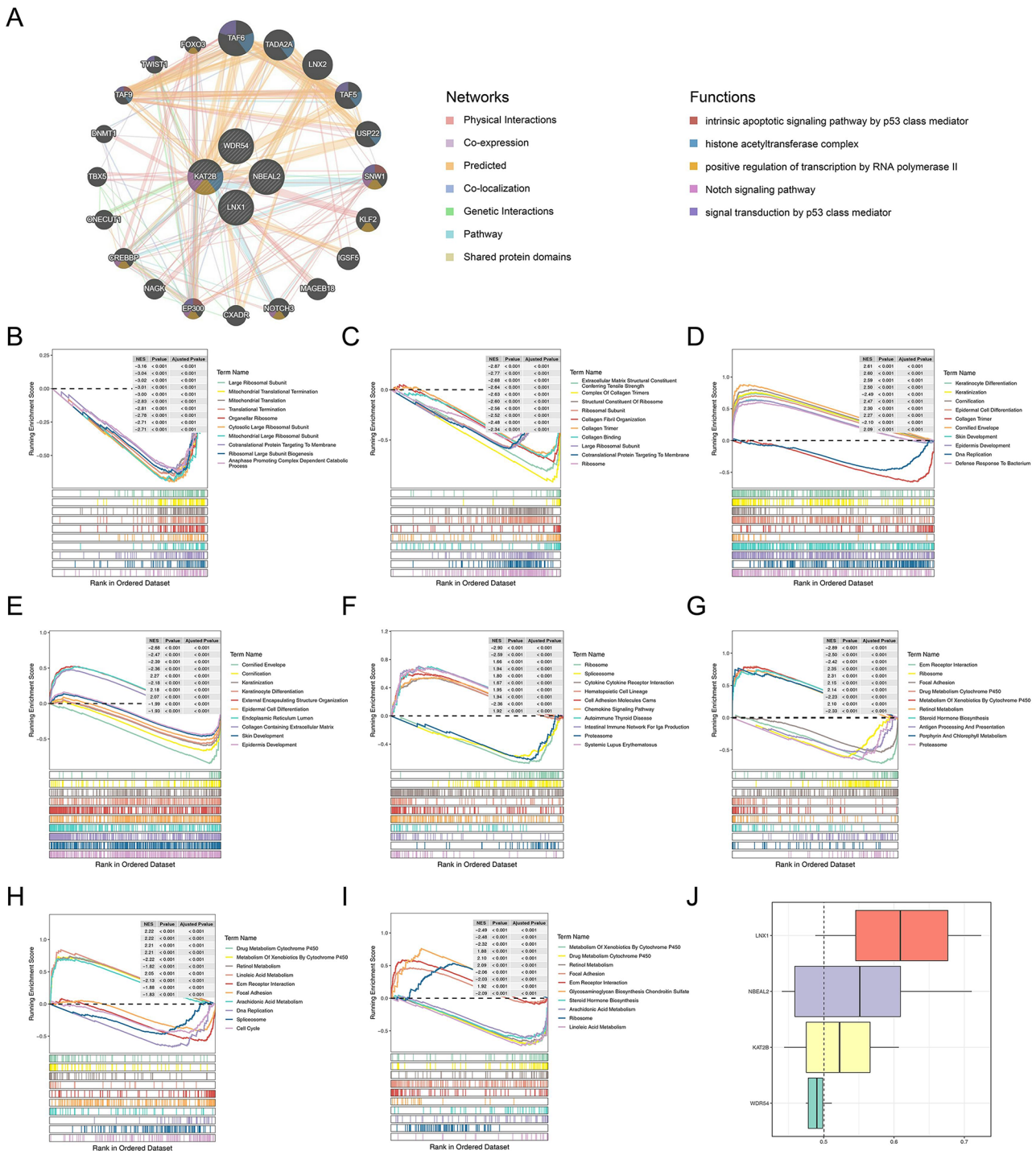


Fig. 7 (A) GeneMANIA enrichment results for biomarkers. (B–I) Results of functional enrichment analysis of biomarkers. (B) KAT2B (C) LNX1 (D) NBEAL2 and (E) WDR54. (F) KAT2B (G) LNX1 (H) NBEAL2 (I) WDR54. (J) Functional similarity scores of biomarkers

with regulatory T cells (Tregs), while memory-resting CD4 T cells were significantly positively correlated with monocytes. Monocytes were also significantly positively correlated with resting dendritic cells. There was a significant negative correlation between M0 macrophages and resting dendritic cells, monocytes, and resting mast cells. Both M1 macrophages and M2 macrophages were significantly positively correlated with resting mast cells (p -value < 0.05) (Fig. 8B). Eight immune cells (memory-resting CD4 T cells, regulatory T cells, monocytes, M0

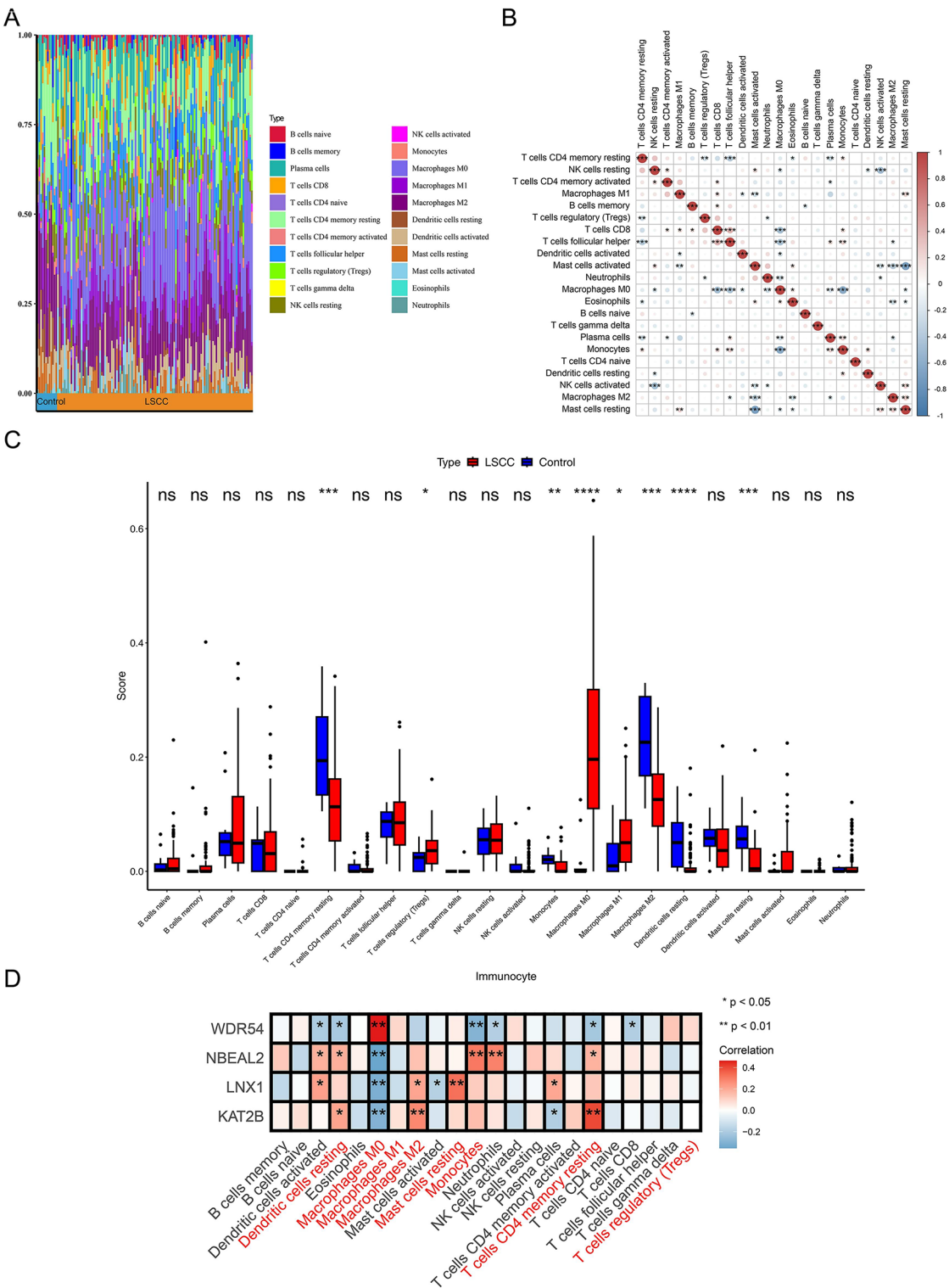


Fig. 8 (A) Heat map of immune cell infiltration. (B) Correlation of immune cells. (C) Box line plot of the difference in immune cell percentage between LSCC and Control groups. (D) Heatmap of correlation between biomarkers and immune cells

macrophages, M1 macrophages, M2 macrophages, resting dendritic cells, and resting mast cells) were significantly different between LSCC and controls (p-value<0.05) (Fig. 8C). Of these, eight immune cells were associated with biomarkers except for M1 Macrophages and regulatory T cells (p-value<0.05) (Fig. 8D).

Biomarkers closely related to cancer and their potential drugs

Biomarker-associated cancer pathways indicated that KAT2B, LNX1, and NBEAL2 were able to activate the majority of cancer-associated pathways, including Hormone AR, Hormone ER, and RAS/MAPK. While WDR54 showed inhibition in PI3K/AKT, RAS/MAPK, RTK, and TSC/mTOR (Fig. 9A). Subsequently,

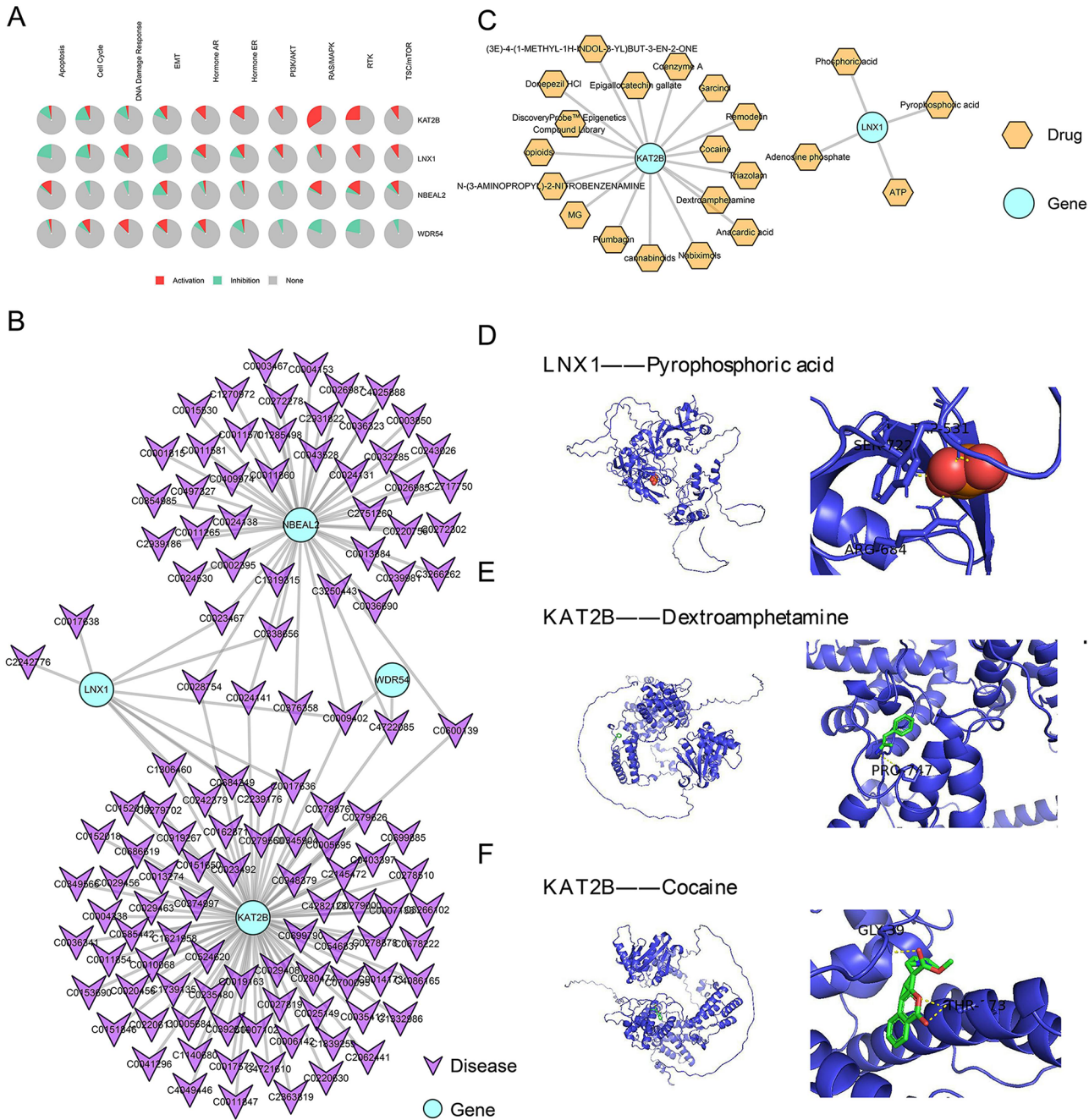


Fig. 9 (A) Role of biomarkers in cancer-related pathways Red is activation, green is inhibition and grey is no effect. (B) Biomarker-disease co-expression network. (C) Biomarker-drug interaction networks. Results of molecular docking simulations of biomarkers. (D) LNX1-Pyrophosphoric acid. (E) KAT2B-Cocaine. (F) KAT2B-Dextroamphetamine

a total of 29 diseases were significantly associated with the biomarkers, the vast majority of which, malignant neoplasms, colorectal carcinoma, neoplasms, primary malignant neoplasm, malignant neoplasm of colon and/or rectum were cancers, further demonstrating that these four biomarkers were strongly associated with cancer (Fig. 9B). Then, KAT2B and LNX1 were predict to be available for targeting drugs. KAT2B was predicted 17 drugs, such as garcinol, cocaine, and triazolam, that could act on LSCC. While LNX1 was predicted ATP, adenosine phosphate, pyrophosphoric acid, and phosphoric acid that might be effective in the subsequent treatment of LSCC patients (Fig. 9C). Finally, only LNX1 and KAT2B were detected as specific drugs. Among them, LNX1 showed standard binding ability to pyrophosphoric acid (affinity = -4.7), mainly to SER-722, ARG-684, and LYS-637 sites (Fig. 9D). KAT2B binds well to PRO-747 on

dextroamphetamine (affinity = -5.6) (Fig. 9E) KAT2B has the strongest binding activity to cocaine (affinity = -7.6) and binds mainly to GLY-39 and THR-573 (Fig. 9F).

Potential molecular mechanisms of LSCC

Only KAT2B and LNX1 were predicted for miRNA and lncRNA. While NBEAL2 was predicted to be regulated by hsa-miR-4717-5p. KAT2B was regulated by four lncRNA. Among them, HCP5 and LINC00598 were jointly involved in miRNA regulation. In contrast, ELFN2 and BDNF-AS were each involved in the regulation of only one miRNA. Expression of hsa-miR-4653-5p and hsa-miR-7162-3p was simultaneously regulated by LINC01556 (Fig. 10A). The degree of KAT2B was much higher than that of other genes, so it was considered a key core gene (Additional file 2). According to ceRNA network theory, interactions between lncRNAs and

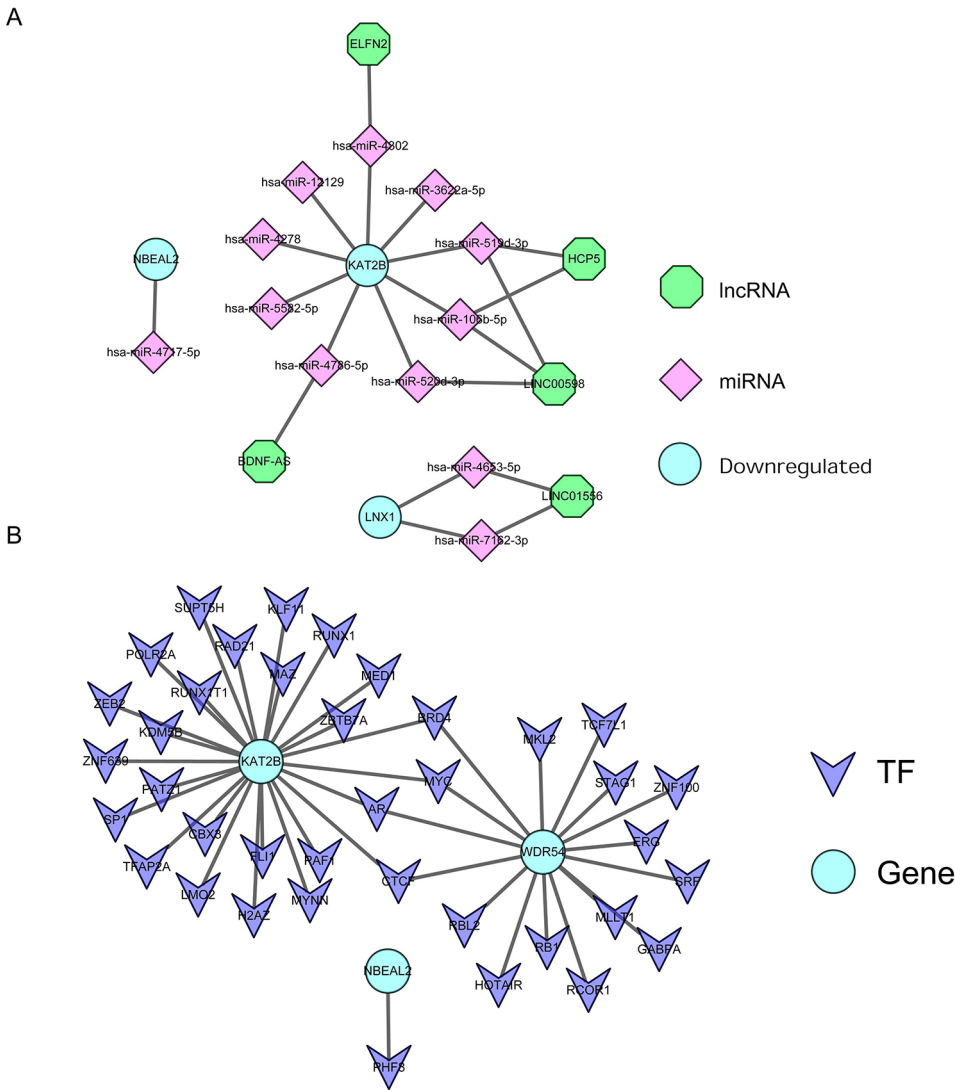


Fig. 10 (A) Biomarker ceRNA regulatory network Biomarkers in powder blue, lncRNAs in green, miRNAs in purple. (B) TF-mRNA regulatory network

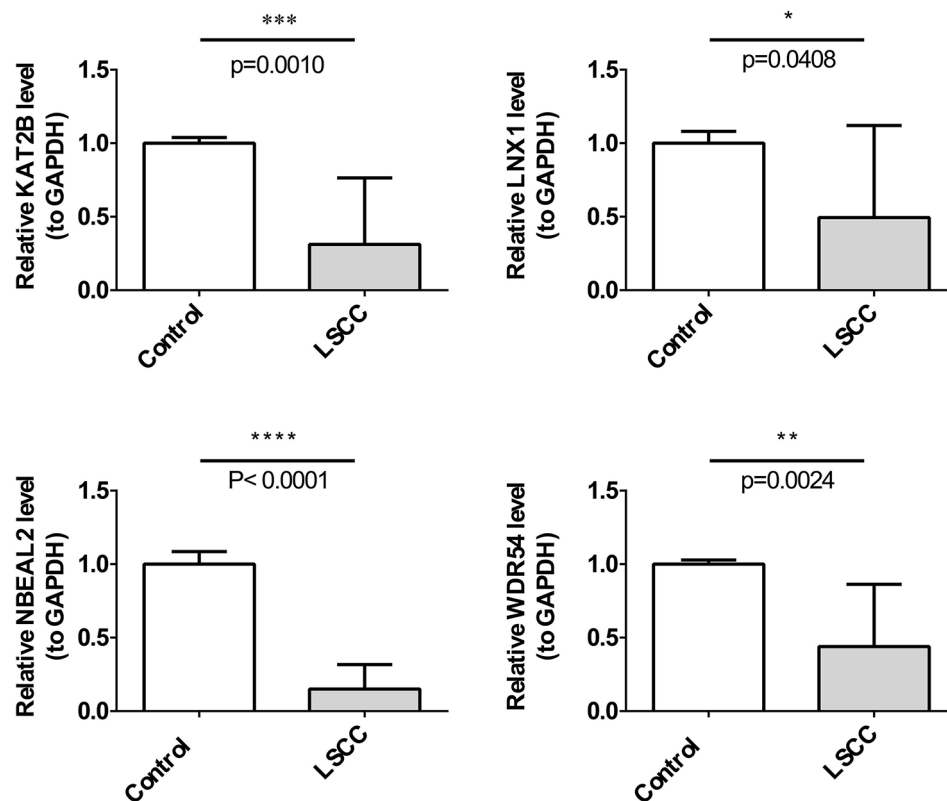


Fig. 11 Biomarker expression validation by RT-qPCR. * $P < 0.05$, ** $P < 0.01$, *** $P < 0.001$, **** $P < 0.001$, ns: non-significance

miRNAs and between miRNAs and mRNAs may exhibit opposite expression patterns. Subsequently, there were 38 TFs with regulatory relationships with biomarkers. Among them, BRD4, MYC, AR, and CTCF were involved in regulating both KAT2B and WDR54 expression. While NBEAL2 was only regulated by PHF8 (Fig. 10B).

Expression validation of biomarkers

We examined the expression of biomarkers by collecting clinical samples using RT-qPCR. The biomarkers were all remarkably expressed between control and disease groups (p -value < 0.05). Among them, KAT2B, LNX1, and NBEAL2 were remarkably lower in the LSCC group, which were consistent with the expression trend in the dataset. WDR54 was notably lower in the disease group, contrary to the expression trend in the dataset, which needed to be revalidated by more experiments (Fig. 11).

Discussion

LSCC has an insidious onset, with 60% of patients diagnosed with advanced disease and low 5-year survival rates. 5-year survival rates, and none of the current treatment options have been able to improve the status quo, highlighting the need for novel biomarkers. Ubiquitination is a post-translational modification, and dysregulation of the ubiquitin-proteasome system (UPS) has

been associated with many cancers, including LSCC [32]. MCTS1 promotes LSCC cell proliferation in part through effects on the ubiquitination and degradation of the OTUD6B-LIN28B axis substrate [33]. Circular RNA MTCL1 promotes the complement C1q-binding protein (C1QBP)-dependent ubiquitin degradation through promotion of dependent ubiquitin degradation, which in turn activates Wnt/ β -catenin signaling, plays a key oncogenic function in laryngeal carcinogenesis and progression [4]. However, the specific molecular mechanisms between the two are not known. Therefore, This study identified WDR54, KAT2B, NBEAL2 and LNX1 as ubiquitination-associated biomarkers in LSCC using transcriptomic analysis and machine learning algorithms and constructed independent prognostic risk models. Biological pathways and regulatory networks were also analyzed for the biomarkers. In order to discover effective new therapeutic targets and provide a theoretical basis for the diagnosis and treatment of patients.

WDR54 promotes cell proliferation by activating AKT, ERK and β -catenin signaling in cancer. Mechanistically, the cross-linking of WDR54 was found to be associated with the ubiquitination response [34]. It was found that the oncogenic circMTCL1 directly binds to the prevalent acid glycoprotein C1QBP and inhibits the ubiquitin degradation of C1QBP, thereby exerting oncogenic functions

in LSCC cells [4]. This suggests that ubiquitination is closely related to the progression of LSCC disease, and that WDR54 may play a role in the proliferation of cells by influencing ubiquitination. This suggests that ubiquitination is closely related to LSCC disease progression and that WDR54 may play a role in LSCC disease progression by affecting ubiquitination [35].

KAT2B, a histone acetyltransferase, is involved in the regulation of gene expression and may influence tumor formation and progression through its acetylation activity. KAT2B is acetylated, and acetylation plays an important role in oral squamous cell carcinoma, not only affecting gene expression and cellular function, but also potentially participating in OSCC progression by regulating the stability and function of specific proteins. Laryngeal squamous cell carcinoma is pathologically identical to OSCC, and KAT2B may play an equivalent mechanism in LSCC [36]. NBEAL2, which plays an important role in platelet generation and functional maintenance. LNX1 has been studied more frequently in gliomas, which may promote glioma progression by modulating tumor cells' life cycle and promote the progression of glioma [37]. However, the functions and roles of NBEAL2 and LNX1 in LSCC have not been reported yet. The analysis in this study revealed that these two biomarkers play an important role in LSCC. This suggests that NBEAL2 and LNX1 may be new potential therapeutic targets for LSCC.

In order to deeply explore the relationship between different genes and clinical features, tumor occurrence, development and metastasis of laryngeal cancer patients, we firstly assessed the diagnostic value of WDR54, KAT2B, NBEAL2 and LNX1 genes using ROC curves, and the results showed good performances in several datasets. Meanwhile, the expression levels of these genes were closely related to tumorigenesis, progression and metastasis. By Wilcoxon test, we found that the expression levels of LNX1 and NBEAL2 predicted poorer prognosis and survival, while the expression of WDR54 was closely related to the number and distribution of lymph node involvement. In addition, the expression levels of different genes may be correlated with the characteristics of tumor cells. To help researchers better understand the heterogeneity of tumors, we constructed high and low expression models based on each marker and found them to have excellent predictive performance. In the KM survival curve analysis of the test and validation sets, our model showed good prognostic results, which supports its potential application in prognostic prediction. In addition, the prognostic model for hepatocellular carcinoma constructed by Yuan et al. based on genes characterized by UbRGs also showed good predictive ability [38]. These findings are consistent with our goal of hypothesizing that UbRGs can serve as reliable tumor prognostic biomarkers. Taken together, these findings suggest

the potential prognostic value of UbRGs-based prediction models in laryngeal cancer and provide a theoretical basis for the development of personalized treatment plans.

GSEA enrichment analysis showed that KAT2B and LNX1 were co-enriched to the Notch signaling pathway. The Notch signaling pathway is a conserved signaling pathway that plays a role in normal biological processes such as cell differentiation, apoptosis and stem cell self-renewal [39]. It plays an important role in organ development and damage repair by regulating cell fate, proliferation and inhibiting terminal differentiation. In LSCC, aberrant activation of the Notch signaling pathway is associated with metabolic reprogramming of tumor cells and may affect cell survival and death. In addition, the Notch signaling pathway plays a key role in epithelial-mesenchymal transition (EMT), which is an important mechanism by which tumor cells acquire malignant properties and affects cell migration. It also has an important role in cell proliferation by affecting metabolic reprogramming of tumor cells, especially during the glycolytic transition [40]. LNX1 and KAT2B have an important impact on cancer cell proliferation, differentiation, and survival by regulating Notch signaling. KAT2B, a histone acetyltransferase, is involved in the regulation of gene expression along with LNX1, affecting the Notch signaling pathway. In the Notch signaling pathway, KAT2B and LNX1 may influence the development of LSCC by affecting the transcriptional activity of specific genes, which in turn may have an impact on the development of LSCC [37, 41, 42].

Immune infiltration analyses showed that LNX1 and KAT2B expression were significantly positively correlated in Macrophages M1; WDR54 was significantly negatively correlated in monocytes, and NBEAL and monocytes were significantly positively correlated. Macrophages are characterized by diversity and plasticity, and M2-type macrophages are associated with anti-inflammatory responses and tissue remodeling [43]. Studies have shown that dysregulation of the salivary microbiota and cytokines affects the development and progression of oral squamous cell carcinoma mainly through inflammation and LSCC is the second most prevalent cancer in the head and neck region after oral squamous cell carcinoma [44]. This suggests that Macrophages M1 may influence the progression of LSCC through anti-inflammatory responses. Monocytes is a kind of key immune cells in human blood that can differentiate into macrophages or dendritic cells and participate in pathogen clearance, immune surveillance and tissue repair [45]. In laryngeal cancer, monocytes are closely related to the immune microenvironment of cancer, and studies have shown that monocytes play a role in tumor progression by differentiating into tumor-associated macrophages,

especially in promoting tumor cell invasion and metastasis [46]. In summary, monocytes play multiple roles in LSCC progression, and by differentiating into different phenotypes of macrophages (e.g., M1 and M2 types), they can influence immune escape and inflammatory responses to tumors, thereby accelerating tumor growth and spread. In view of this, the differential expression of LNX1, KAT2B, WDR54, and NBEAL2 in monocyte-associated pathways may make them potential LSCC biomarkers. The high expression of LNX1 and KAT2B is positively correlated with M1 macrophages, which may promote anti-tumor inflammatory responses, whereas the opposing regulatory relationships of WDR54 and NBEAL2 with monocytes suggest that they WDR54 and NBEAL2 have opposite regulatory relationships with monocytes, suggesting that they may play roles in different immunoregulatory mechanisms [43, 44].

In drug screening, LNX1 serves as a biomarker associated with cell signaling and transcriptional regulation. Predicted drugs include phosphate, pyrophosphate, and adenine nucleoside triphosphate (ATP). These small molecules play important roles in cellular metabolism, especially in energy transfer and signaling. It has been shown in the literature that changes in ATP are closely related to cell proliferation and apoptosis, so LNX1 may be involved in the progression of diseases such as cancer by affecting the metabolism of these small molecules [47]. KAT2B is a histone acetyltransferase, which is closely related to the regulation of gene expression. Predicted drugs such as cocaine, amphetamines, and triazolam act primarily on the nervous system and may be related to the role of KAT2B in regulating neurotransmitter release and neuroplasticity. In addition, coenzyme A, cannabis extracts and green tea polyphenols are increasingly being studied in tumors and metabolic diseases, suggesting that KAT2B may be a potential target for the actions of these compounds [48, 49]. LNX1 docking drug by regulating intracellular energy status, phosphoric acid may inhibit tumor cell growth while modulating signaling pathways related to cell proliferation and apoptosis, pyrophosphoric acid may regulate LSCC cell proliferation by affecting cellular metabolic pathways, which in turn affects tumor progression. KAT2B docking drug cocaine may alter histone acetylation by affecting the activity of KAT2B status, further regulating the expression of tumor-related genes, and dextroamphetamine may regulate the proliferation and survival of LSCC tumor cells by affecting KAT2B-related signaling pathways.

In the study of cisplatin resistance in HNSCC, BRD4 recognizes and binds to acetylated histones through its bromodomain, promoting the transcription of key oncogenes such as C-MYC, thereby accelerating the proliferation and development of tumor cells [50]. It may also help tumor cells evade the cytotoxicity of chemotherapy drugs

by promoting DNA damage repair. Inflammatory factors may also activate BRD4, leading to chromatin remodeling and resistance to BET inhibitors [51]. The study also mentioned that WDR54 and KAT2B may play a role in laryngeal squamous cell carcinoma through the regulatory action of BRD4, but the specific mechanism is still unclear and further research is needed.

In this study, four LSCC-related ubiquitinated biomarkers, LNX1, NBEAL2, WDR54 and KAT2B, were identified through a series of bioinformatics identifications. Focused on the ubiquitination process and closely linked it to the mechanism of LSCC development, revealing the critical role of ubiquitination regulation in laryngeal cancer. To our knowledge, this is the first study to identify biomarkers associated with ubiquitination in LSCC, but there are still some limitations that may affect the wide application of the results. First, sample selection may lead to selectivity bias, and the size and source of the study sample may not be sufficiently representative, especially in patient populations with different regions, ethnicities, or clinical stages, and the results of the selected samples may not fully reflect the characteristics of the entire LSCC patient population. Second, in addition to ubiquitination markers, other potential confounding factors, such as patients' lifestyles, dietary habits, and smoking and drinking histories, may be closely associated with the onset and progression of LSCC, and these factors may influence the expression of ubiquitination markers. If these factors are not adequately controlled, they may lead to confounding effects and affect the understanding of the relationship between ubiquitination markers and tumor biology. Therefore, the clinical application of biomarkers still needs to be supported by larger studies and data. Meanwhile, the development of drugs targeting these markers also requires further clinical trials to validate their efficacy and safety. In the future, we will further expand the sample size to validate the clinical application potential of these markers and explore therapeutic strategies targeting ubiquitination-related genes. Meanwhile, the biological functions of these genes and their potential roles in the ceRNA network can be verified by Western blot, RNA interference and other techniques.

Conclusions

In this study, four biomarkers (WDR54, KAT2B, NBEAL2 and LNX1) associated with ubiquitination were identified and independent prognostic risk models were constructed. These markers provide new ideas for early diagnosis and precision treatment of LSCC and provide important clues to unravel the molecular mechanisms of LSCC. Although the clinical applications of these markers still need to be further validated, they undoubtedly provide a new research direction for precision treatment

of LSCC and in-depth understanding of the biological mechanisms.

Abbreviations

LSCC	Laryngeal Squamous Cell Carcinoma
UbRGs	Ubiquitination-Related Genes
DEGs	Differentially Expressed Genes
WGCNA	Weighted Gene Co-Expression Network Analysis
RT-qPCR	Reverse Transcription-Quantitative PCR
ROC	Receiver Operating Characteristic
TF	Transcription Factor
HPV	Human Papillomavirus
circMTCL1	Microtubule Cross-Linking Factor 1 circRNA
C1QBP	C1q-Binding Protein
TCGA	The Cancer Genome Atlas
OS	Overall Survival
GEO	Gene Expression Omnibus
DFS	Disease-Free Survival
iUUCD	Integrated Annotations for Ubiquitin and Ubiquitin-like Conjugation Database
LASSO	Least Absolute Shrinkage and Selection Operator
AUC	Area Under Curve
K-M	Kaplan-Meier
GGI	Gene-Gene Interaction
GO	Gene ontology
KEGG	Kyoto Encyclopedia of Genes and Genomes
DisGeNET	Disease Gene Network
LEPR	Leptin Receptor
GeneCrads	Area Under Curve
ceRNA	competing endogenous RNA
UPS	Ubiquitin-Proteasome System
ATP	Adenine Nucleoside Triphosphate
KEGG	Kyoto Encyclopedia of Genes and Genomes
DisGeNET	Disease Gene Network
LEPR	leptin receptor

Supplementary Information

The online version contains supplementary material available at <https://doi.org/10.1186/s12920-025-02148-x>.

Supplementary Material 1: Additional files 1: The list of genes corresponding to each module.

Supplementary Material 2: Additional file 2: The result of ceRNA network analysis.

Acknowledgements

We thank the TCGA and GEO databases and other groups for providing invaluable datasets for statistical analyses.

Author contributions

Each author contributed a significant scholarship to this manuscript. Research designed and study, prepared and figures: CQ, MYF and WZM. Prepared figures, collection and analyzed data: CQ and WZM. Manuscript writing-original draft preparation and conceptualization: CQ. Manuscript writing-review and editing: MYF.

Funding

This study was supported by the [National Natural Science Foundation of China] under grant agreement number [82260541] and Guizhou Provincial Health Commission Foundation [gzwkj2025-435].

Data availability

No datasets were generated or analysed during the current study.

Declarations

Ethics approval and consent to participate

This study was conducted in full compliance with the principles outlined in the Declaration of Helsinki and all applicable ethical guidelines. Ethical

approval for this research was obtained from the Medical Science Ethics Committee of the Affiliated Hospital of Guizhou Medical University, with approval number 2022 (221). All participants were provided with detailed information regarding the purpose, procedures, and potential risks of the study prior to their involvement. Written informed consent was obtained from each participant before their participation in the research.

Consent for publication

Not Applicable.

Competing interests

The authors declare no competing interests.

Author details

¹School of Clinical Medicine, Guizhou Medical University, Guiyang, Guizhou 550004, China

²Department of Otorhinolaryngology, Affiliated Hospital of Guizhou Medical University, 28 Guiyi Street, Yunyan District, Guiyang, Guizhou 550004, China

Received: 19 March 2025 / Accepted: 21 April 2025

Published online: 12 May 2025

References

- He Y, Liang D, Li D, Shan B, Zheng R, Zhang S, et al. Incidence and mortality of laryngeal cancer in China, 2015. *Chin J Cancer Res.* 2020;32(1):10–7.
- Carlisle JW, Steuer CE, Owonikoko TK, Saba NF. An update on the immune landscape in lung and head and neck cancers. *CA Cancer J Clin.* 2020;70(6):505–17.
- De Silva ARI, Page RC. Ubiquitination detection techniques. *Exp Biol Med (Maywood).* 2023;248(15):1333–46.
- Wang Z, Sun A, Yan A, Yao J, Huang H, Gao Z, et al. Circular RNA MTCL1 promotes advanced laryngeal squamous cell carcinoma progression by inhibiting C1QBP ubiquitin degradation and mediating beta-catenin activation. *Mol Cancer.* 2022;21(1):92.
- Wang QD, Shi T, Xu Y, Liu Y, Zhang MJ. USP21 contributes to the aggressiveness of laryngeal cancer cells by deubiquitinating and stabilizing AURKA. *Kaohsiung J Med Sci.* 2023;39(4):354–63.
- Fountzilas E, Kotoula V, Angouridakis N, Karasmanis I, Wirtz RM, Eleftheraki AG, et al. Identification and validation of a multigene predictor of recurrence in primary laryngeal cancer. *PLoS ONE.* 2013;8(8):e70429.
- Zheng X, Gao W, Zhang Z, Xue X, Mijiti M, Guo Q, et al. Identification of a seven-lncRNAs panel that serves as a prognosis predictor and contributes to the malignant progression of laryngeal squamous cell carcinoma. *Front Oncol.* 2023;13:1106249.
- Love MI, Huber W, Anders S. Moderated Estimation of fold change and dispersion for RNA-seq data with DESeq2. *Genome Biol.* 2014;15(12):550.
- Langfelder P, Horvath S. WGCNA: an R package for weighted correlation network analysis. *BMC Bioinformatics.* 2008;9:559.
- Wu T, Hu E, Xu S, Chen M, Guo P, Dai Z, et al. ClusterProfiler 4.0: A universal enrichment tool for interpreting omics data. *Innov (Camb).* 2021;2(3):100141.
- Friedman J, Hastie T, Tibshirani R. Regularization paths for generalized linear models via coordinate descent. *J Stat Softw.* 2010;33(1):1–22.
- Geng R, Huang X, Li L, Guo X, Wang Q, Zheng Y, et al. Gene expression analysis in endometriosis: immunopathology insights, transcription factors and therapeutic targets. *Front Immunol.* 2022;13:1037504.
- Maurya NS, Kushwah S, Kushwaha S, Chawade A, Mani A. Prognostic model development for classification of colorectal adenocarcinoma by using machine learning model based on feature selection technique Boruta. *Sci Rep.* 2023;13(1):6413.
- Robin X, Turck N, Hainard A, Tiberti N, Lisacek F, Sanchez JC, et al. pROC: an open-source package for R and S+ to analyze and compare ROC curves. *BMC Bioinformatics.* 2011;12:77.
- Liu TT, Li R, Huo C, Li JP, Yao J, Ji XL, et al. Identification of CDK2-Related immune forecast model and CeRNA in lung adenocarcinoma, a Pan-Cancer analysis. *Front Cell Dev Biol.* 2021;9:682002.
- Zhang H, Meltzer P, Davis S. RCircos: an R package for circos 2D track plots. *BMC Bioinformatics.* 2013;14:244.

17. Safran M, Dalah I, Alexander J, Rosen N, Iny Stein T, Shmoish M, et al. GeneCards version 3: the human gene integrator. *Database (Oxford)*. 2010;2010:baq020.
18. Wu C, Jin X, Tsueng G, Afrasiabi C, Su AI. BioGPS: Building your own mash-up of gene annotations and expression profiles. *Nucleic Acids Res*. 2016;44(D1):D313–6.
19. Qing J, Li C, Hu X, Song W, Tirichen H, Yaigoub H, et al. Differentiation of T helper 17 cells may mediate the abnormal humoral immunity in IgA nephropathy and inflammatory bowel disease based on shared genetic effects. *Front Immunol*. 2022;13:916934.
20. Yu G. Gene ontology semantic similarity analysis using gosemsim. *Methods Mol Biol*. 2020;2117:207–15.
21. Liu CJ, Hu FF, Xia MX, Han L, Zhang Q, Guo AY. GSCALite: a web server for gene set cancer analysis. *Bioinformatics*. 2018;34(21):3771–2.
22. Pineri J, Ramirez-Anguita JM, Sauch-Pitarch J, Ronzano F, Centeno E, Sanz F, et al. The disgenet knowledge platform for disease genomics: 2019 update. *Nucleic Acids Res*. 2020;48(D1):D845–55.
23. Fishilevich S, Zimmerman S, Kohn A, Iny Stein T, Olender T, Kolker E et al. Genic insights from integrated human proteomics in GeneCards. *Database (Oxford)*. 2016;2016.
24. Saikia S, Bordoloi M. Molecular docking: challenges, advances and its use in drug discovery perspective. *Curr Drug Targets*. 2019;20(5):501–21.
25. Dweep H, Gretz N, Sticht C. MiRWalk database for miRNA-target interactions. *Methods Mol Biol*. 2014;1182:289–305.
26. Wong N, Wang X. MiRDB: an online resource for MicroRNA target prediction and functional annotations. *Nucleic Acids Res*. 2015;43(Database issue):D146–52.
27. Chou CH, Chang NW, Shrestha S, Hsu SD, Lin YL, Lee WH, et al. MiRTarBase 2016: updates to the experimentally validated miRNA-target interactions database. *Nucleic Acids Res*. 2016;44(D1):D239–47.
28. Karagkouni D, Paraskevopoulou MD, Chatzopoulos S, Vlachos IS, Tastsoglou S, Kanellos I, et al. DIANA-TarBase v8: a decade-long collection of experimentally supported miRNA-gene interactions. *Nucleic Acids Res*. 2018;46(D1):D239–45.
29. Salmena L, Poliseno L, Tay Y, Kats L, Pandolfi PP. A CeRNA hypothesis: the Rosetta stone of a hidden RNA language? *Cell*. 2011;146(3):353–8.
30. Wu X, Sui Z, Zhang H, Wang Y, Yu Z. Integrated analysis of lncRNA-Mediated CeRNA network in lung adenocarcinoma. *Front Oncol*. 2020;10:554759.
31. Li T, Fu J, Zeng Z, Cohen D, Li J, Chen Q, et al. TIMER2.0 for analysis of tumor-infiltrating immune cells. *Nucleic Acids Res*. 2020;48(W1):W509–14.
32. Gao L, Zhang W, Shi XH, Chang X, Han Y, Liu C, et al. The mechanism of linear ubiquitination in regulating cell death and correlative diseases. *Cell Death Dis*. 2023;14(10):659.
33. Ma B, Wei X, Zhou S, Yang M. MCTS1 enhances the proliferation of laryngeal squamous cell carcinoma via promoting OTUD6B-1 mediated LIN28B deubiquitination. *Biochem Biophys Res Commun*. 2023;678:128–34.
34. Wei X, Wang B, Wu Z, Yang X, Guo Y, Yang Y, et al. WD repeat protein 54-mediator of ErbB2-driven cell motility 1 axis promotes bladder cancer tumorigenesis and metastasis and impairs chemosensitivity. *Cancer Lett*. 2023;556:216058.
35. Hayes PD, Nasim A, London NJ, Sayers RD, Barrie WW, Bell PR, et al. In situ replacement of infected aortic grafts with rifampicin-bonded prostheses: the Leicester experience (1992 to 1998). *J Vasc Surg*. 1999;30(1):92–8.
36. Silva LC, Leite AA, Borgato GB, Wagner VP, Martins MD, Loureiro FJA, et al. Oral squamous cell carcinoma cancer stem cells have different drug sensitive to Pharmacological NF κ B and histone deacetylation Inhibition. *Am J Cancer Res*. 2023;13(12):6038–50.
37. Baisiwala S, Hall RR 3rd, Saathoff MR, Park JMS, Budhiraja C. S, LNX1 modulates Notch1 signaling to promote expansion of the glioma stem cell population during Temozolomide therapy in glioblastoma. *Cancers (Basel)*. 2020;12(12).
38. Yuan Z, Zhu Q, Wu Q, Zhang Z, Guo J, Wu G, et al. Prognostic and immune landscape analysis of Ubiquitination-related genes in hepatocellular carcinoma: based on bulk and Single-cell RNA sequencing data. *J Cancer*. 2024;15(9):2580–600.
39. Shim YS, Lee HS, Hwang JS. Aberrant Notch signaling pathway as a potential mechanism of central precocious puberty. *Int J Mol Sci*. 2022;23(6).
40. Wang X, Tian L, Li Y, Wang J, Yan B, Yang L, et al. RBM15 facilitates laryngeal squamous cell carcinoma progression by regulating TMBIM6 stability through IGF2BP3 dependent. *J Exp Clin Cancer Res*. 2021;40(1):80.
41. Bekri A, Liao M, Drapeau P. Glycine regulates neural stem cell proliferation during development via Lnx1-Dependent Notch signaling. *Front Mol Neurosci*. 2019;12:44.
42. Feng C, Xiong Z, Jiang H, Ding Q, Fang Z, Hui W. Genetic alteration in Notch pathway is associated with better prognosis in renal cell carcinoma. *BioFactors*. 2016;42(1):41–8.
43. Wang LX, Zhang SX, Wu HJ, Rong XL, Guo J. M2b macrophage polarization and its roles in diseases. *J Leukoc Biol*. 2019;106(2):345–58.
44. Rai AK, Panda M, Das AK, Rahman T, Das R, Das K, et al. Dysbiosis of salivary Microbiome and cytokines influence oral squamous cell carcinoma through inflammation. *Arch Microbiol*. 2021;203(1):137–52.
45. Regal-McDonald K, Patel RP. Selective recruitment of monocyte subsets by endothelial N-Glycans. *Am J Pathol*. 2020;190(5):947–57.
46. Li JD, Chen Y, Jing SW, Wang LT, Zhou YH, Liu ZS, et al. Triosephosphate isomerase 1 May be a risk predictor in laryngeal squamous cell carcinoma: a multi-centered study integrating bulk RNA, single-cell RNA, and protein immunohistochemistry. *Eur J Med Res*. 2023;28(1):591.
47. Jang M, Park R, Park YI, Park Y, Lee JI, Namkoong S et al. LNX1 contributes to cell cycle progression and cisplatin resistance. *Cancers (Basel)*. 2021;13(16).
48. Wharen R. Clinical effects of deep brain stimulation on gait disorders in Parkinson's disease. *Eur J Neurol*. 2010;17(5):639–40.
49. Howland-Gradman J, Broderick S. Soar to excellence with rapid feedback and rapid response. *Nurs Manage*. 2002;33(2):43.
50. Lima de Oliveira J, More Milan T, Longo Bighetti-Trevisan R, Fernandes RR, Machado Leopoldino A, Oliveira de Almeida L. Epithelial-mesenchymal transition and cancer stem cells: A route to acquired cisplatin resistance through epigenetics in HNSCC. *Oral Dis*. 2023;29(5):1991–2005.
51. Milan TM, Eskenazi APE, Bighetti-Trevisan RL, de Almeida LO. Epigenetic modifications control loss of adhesion and aggressiveness of cancer stem cells derived from head and neck squamous cell carcinoma with intrinsic resistance to cisplatin. *Arch Oral Biol*. 2022;141:105468.

Publisher's note

Springer Nature remains neutral with regard to jurisdictional claims in published maps and institutional affiliations.